A Novel Steerable Filter in the Frequency Domain: The Rose Curve Filter

Ömer MİNTEMUR[1], Hilal KAYA[1], Recep DEMİRCİ[2]
[1]*Ankara Yıldırım Beyazıt University, Faculty of Engineering and Natural Sciences, Computer Engineering Department, Turkey*
[2]*Gazi University, Faculty of Technology, Computer Engineering Department, Turkey*
omintemur@ybu.edu.tr

***Abstract*—Feature extraction in image processing is a difficult task. To do this, a filter bank is one of the most used techniques. To extract a feature, the image is masked with filters in prepared filter banks, one by one. If a greater number of features can be extracted from an image, the task is easier. Thus, identifying more features is desirable in many image processing applications. However, filter preparation can be troublesome because of the difficulties in determining a filter's parameters such as direction. Limitations of the selected filter are another issue. Thus, an easy-to-use filter with few parameters and directional flexibility is a desirable choice. For these reasons, a novel steerable type of filter is proposed in this study. The proposed rose curve filter uses Lemniscate shapes derived from the rose curves to extract image features in the frequency domain. It has three parameters, fewer than other filters, and has directional flexibility. It can also extract images in more than one direction. Experimental results show that it is effective in feature extraction during image processing.**

***Index Terms*—feature extraction, filtering, Fourier transforms, image processing, pattern recognition.**

I. INTRODUCTION

Understanding a scene or an image for humans is an easy task since our perception system can easily recognize details and deduce meaning. However, the same process is difficult for computers and not automatic. Computers must firstly extract image features before further processing. An image feature can be described by the information it contains such as color and shape [1-2] in addition to statistical features [3-4]. Although statistical features can contribute to feature extraction, more features can be extracted based on the shape. Shape-based feature extraction is based on filters, also called masks, which allow edges or directional features to be extracted. These methods can resolve more concrete features than the statistical approaches and are widely used [5–7]. Due to the rapid development of the technology, feature extraction has become relatively easy and new methods are proposed continuously. During feature extraction, a filter or filter bank, which comprises a set of filters, is applied to an image. These filters extract directional information, which is an important aspect in feature extraction process. Since spatial filtering and identifying spatial direction is difficult, filtering the frequency domain is best approach for both speed and direction. Many methods have been proposed for extracting directional features in the frequency domain. These methods are generally based on the partition of the frequency domain, first proposed by [8]. Generally, a set of filters are prepared and applied to an image and transformed into the frequency domain. These filters are called directional filter banks (DFBs). More recently, derivatives for partitioning the frequency domain have been proposed for directional feature extraction. This is an active area of image processing researches [9-15].

Extracted features are processed and fed into a machine learning algorithm for classification [16–18]. Machine learning algorithms require many data, which are important for accurately extracting features with filters. Besides feature extraction, DFBs are used in other image processing areas such as denoising [19-21], watermark embedding [22] and detection [23], image fusion [24], and reconstruction [25].

Most filters are diamond-shape wedges, which are also called square or fan filters. When directionality is an issue, the steering ability of these filters is limited. Filter shape is fixed and cannot be easily changed, calculations for preparing these filters are complex [14], their parameters are not simple, and it is difficult to combine other filters. These are important limitations of the square or the fan filters because angle flexibility and simplicity are important during feature extraction.

With these considerations in mind, this study proposes a novel steerable filter based on the rose curve (see preliminary results in [26]). In summary, the contributions of the study are:

- A new frequency filter based on the Lemniscate version of the rose curve for feature extraction is proposed.
- The new filter for feature extraction has only three easily adjustable parameters.
- The proposed mechanism is validated on sample images.
- The proposed mechanism performance is tested on facial expression classification problem.
- Results suggest that the filter can be used for feature extraction in image processing applications.

The organization of the paper is as follows: section 2 explains frequency domain filtering with Gaussian high pass filters and provides details on the proposed filter. Section 3 is divided into two subsections. In first subsection, the proposed method for feature extraction mechanism is tested qualitatively on the images of Lena, the Cameraman, and a human retina. In second subsection, features extracted using the proposed feature extraction mechanism are used in facial expression recognition (FER) classification. The last section provides concluding remarks and suggestions for future research.

Digital Object Identifier 10.4316/AECE.2021.02006

II. Frequency Domain Image Filtering

Image filtering processes a two-dimensional array to attain features in an image such as edges, lines, circles, and textures. This can be done in the spatial or frequency domain. It may not be easy to detect object boundaries or repeated patterns using spatial algorithms. However, the Fourier domain provides more information on edges and sharper transitions, hence feature extraction is widely done in the frequency domain.

A. 2D Fourier Transform

The 2D Fourier transform [27] is used in many applications from signal processing to image processing, based on Joseph Fourier's work showing that any periodic phenomena can be represented as sine and cosine functions. Fourier transforms convert waveforms to alternative waveforms in the frequency domain. In image processing, the 2D Fourier transform is defined as follows:

$$F(u,v)=\sum_{x=0}^{M-1}\sum_{y=0}^{N-1}f(x,y)e^{-2i\pi(\frac{ux}{M}+\frac{vy}{N})} \quad (1)$$

where, u represents horizontal frequency and v represents vertical frequency. *F(u, v)* is a complex array with the same image size.

Fig. 1 shows the Cameraman, a popular test image and Fig. 2 shows its Fourier coefficients. In the Fourier domain, a plane can be divided into two sections, horizontal–vertical or low–high frequencies. Towards the middle, low frequencies dominate the plane where there are smooth transitions in the spatial domain. Towards the edges, high frequencies dominate the plane where there are sharp transitions in the spatial domain. These two Fourier transform features are very important for filtering and extracting features. The 2D Fourier transform is faster than spatial domain filtering. After filtering, the image is transformed back into the spatial domain with the inverse Fourier transform:

$$f(x,y)=\frac{1}{MN}\sum_{u=0}^{M-1}\sum_{v=0}^{N-1}F(u,v)e^{2i\pi(\frac{ux}{M}+\frac{vy}{N})} \quad (2)$$

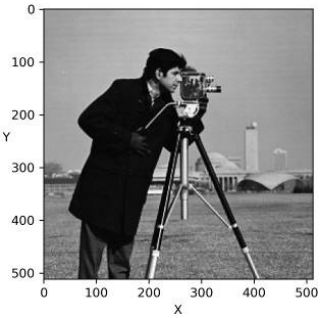

Figure 1. Original cameraman image

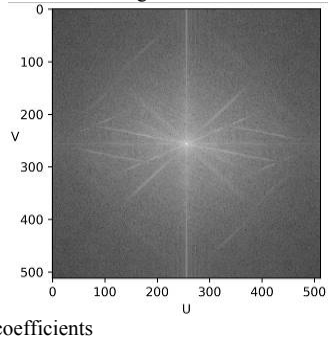

Figure 2. Fourier coefficients

B. Gaussian High Pass Filter

Frequency domain image filtering is done by processing Fourier coefficients and this depends on partitioning the frequency domain. High and low pass filters preserve high and low frequencies, respectively. One example of a high pass filter is the Gaussian high pass filter:

$$H(u,v)=1-e^{-D^2(u,v)/2D_0^2} \quad (3)$$

where, D_0 is the cutting frequency radius. $D(u,v)$ is the Euclidean distance between any point on the $u-v$ plane, which can be restated as:

$$D(u,v)=\sqrt{(u-\frac{M}{2})^2+(v-\frac{N}{2})^2} \quad (4)$$

Descriptive features can be better extracted from higher frequencies since lower frequencies may not contain much information on edges, corners, and lines. Gaussian high pass filters attenuate low frequencies, allowing high frequency to pass, and do not suffer from the ringing effect produced by the ideal high pass filter. Fig. 3 shows Gaussian high pass filters of the Cameraman image and its responses in the spatial domain.

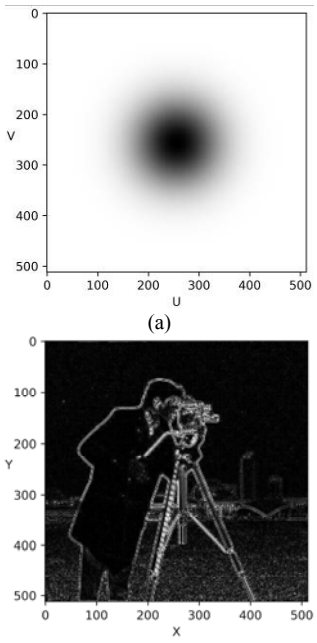

Figure 3. (a) Gaussian high pass filter (D_0 = 60) (b) spatial response

Since all frequencies outside the circle's radius can pass through, this filter has no specified direction. However, certain applications require detecting angled features. Since targeted features may lie in a specific direction, so steerable filters are crucial in feature extraction.

Many methods have been proposed to make steerable filters such as the Contourlet transform [11]. However, since it uses directional frequency partitioning, proposed by [8], only certain angles can be selected. Also, Contourlet transforms only extract one direction in one filter. A variant, the Curvelet transform [15], has the same issues. These are built-in filters and often used as is or with minor modifications. In Contourlet transform generally the frequency plane is divided into 4 or 8 sub-bands to extract features. Without control over filter direction, feature extraction is inefficient. Another widely-used directional filter is the 2D Gabor filter [28], but it has issues such as

myriad but constrained parameters [29]. For all three of these filters, a new filter must be prepared for each direction.

To address these shortcomings, we propose new rose curve filter for feature extraction. The directional characteristic of the rose curve makes this shape especially suitable. Used as a filter for image processing, this shape has fewer parameters and more freedom to combine with different high pass filters. Unlike other filters, the rose curve filter can extract features from various directions by adjusting a single parameter, the number of leaves.

C. Feature Extraction with Rose Curves

The rose curve is a Polar coordinate version of a sinusoid plotted in the Cartesian coordinate system. The curve was named by Italian mathematician Guido Grandi, referring to the rose shape of the sinusoid in the polar coordinate system. In this system, a typical curve could be defined as:

$$r = a * \cos(k * \theta) \tag{5}$$

where, a represents the length of a leaf, k represents the number of the leaves, and θ is the angle in the polar coordinate system. Fig. 4 shows the curve using (5). If the polar coordinate system and frequency domain system or $u-v$ plane are overlapped, the angle in the polar system can be restated as follows:

$$\theta = \tan^{-1}(v/u) \tag{6}$$

Although different kinds of curves can be drawn, the Lemniscate is preferred because its symmetry makes it compatible with the structure of the frequency domain. The general definition of a Lemniscate is as follows:

$$r^2 = a^2 * \cos(2 * \theta) \tag{7}$$

The conventional Lemniscate has only two symmetrical leaves (Fig. 5). We added a new angle parameter β, making this a steerable or rotatable Lemniscate:

$$r^2 = a^2 * \cos(2 * \theta + 2 * \beta) \tag{8}$$

Infinite Lemniscate curves could be obtained by changing the angle; Fig. 6 only shows the angles of 0°, 45°, 90°, and 135°. It is important that Fourier domain filters are symmetric around the frequency plane origin. This curve's symmetry does not change when it is rotated.

When rose curves are overlaid on a frequency plane, regions occupied by the curves can be used to select the desired frequency components in the image. If the Lemniscate curve is used, any region of frequency domain could be chosen by rotating the Lemniscate. Hence, this is a steerable filter in the frequency domain. Furthermore, a high pass filter, such as the Gaussian filter used here, can be integrated (Fig. 7).

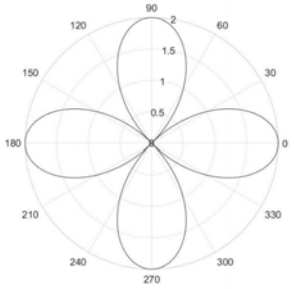

Figure 4. Rose curve for Equation 5: $a = 2$ and $k = 4$

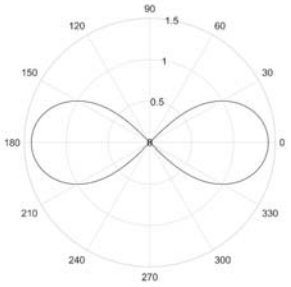

Figure 5. The Lemniscate, $a = 2$

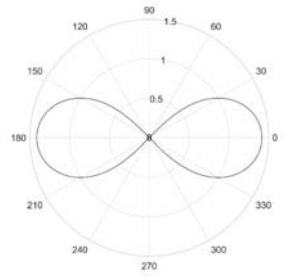

(a)

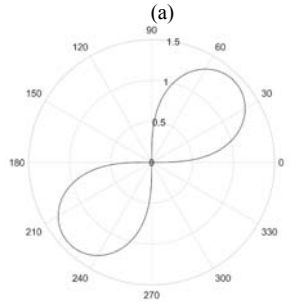

(b)

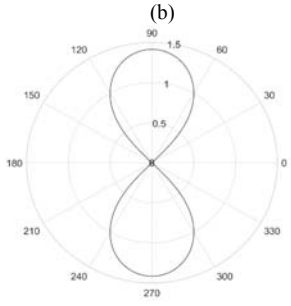

(c)

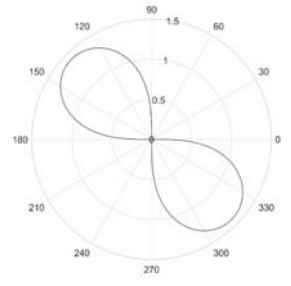

(d)

Figure 6. Rotated Lemniscate curves: a = 2, β = (a) 0°, (b) 45°, (c) 90°, (d) 135°

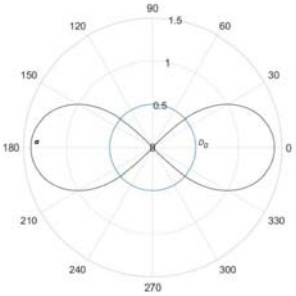

Figure 7. Lemniscate curve filter and high pass filter. The cutting frequency is a circle with radius D_0

It is possible to attain different filtering characteristics with different curves. Since the ideal high pass filter suffers from the ringing problem, this study uses a Gaussian high pass filter to overcome this problem. Since sharp transitions occur at the edges of Lemniscate curves, a Gaussian band pass filter can be used to smooth the transition (Fig. 8). The Gaussian band pass controls the transition region, so the transition band at the edges of the Lemniscate is similar to the Gaussian band pass transition. The frequency response of the proposed filter is given in Fig. 9. An image filtering flow chart for the new filter is shown in Fig. 10.

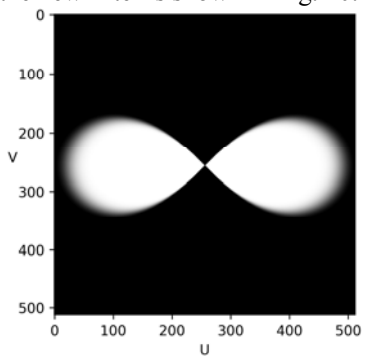

Figure 8. Lemniscate curve with Gaussian band pass at the edges

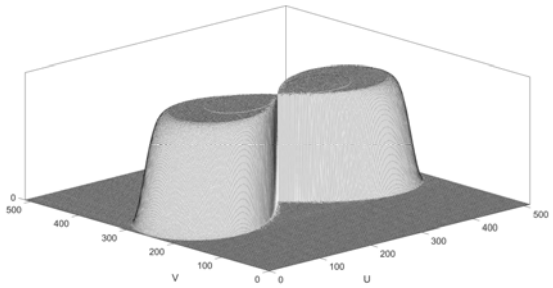

Figure 9. Frequency response of proposed filter

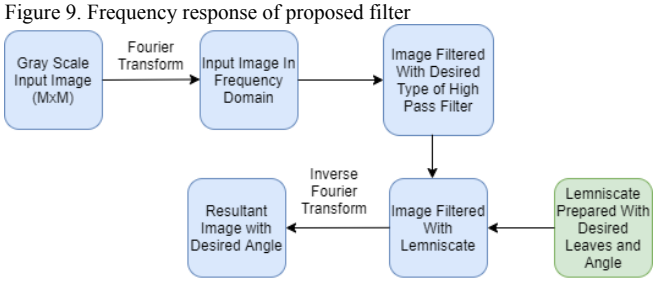

Figure 10. Image filtering flow chart with the Lemniscate

III. Experimental Results And Discussion

Performance of the feature extraction method with the proposed filter was tested both qualitatively and quantitatively. Next two subsections present and discuss the results obtained both qualitatively and quantitatively respectively.

A. Qualitative Performance

For qualitative performance, proposed method was tested with the well-known Lena Fig.11 (a) and Cameraman images. As an example of a practical application, it was also tested with a sample retina image Fig.11 (b). All images are grayscale and have a size of 512×512 pixels. A Gaussian high pass response of the images of Lena and the retina were obtained using $D_0 = 60$ (Fig. 12).

Unlike other filters, the rose curve filter can extract directional features. The curve can be rotated at any angle and thereby cover any frequency region; here we only show four angles: 0°, 45°, 90°, and 135°.

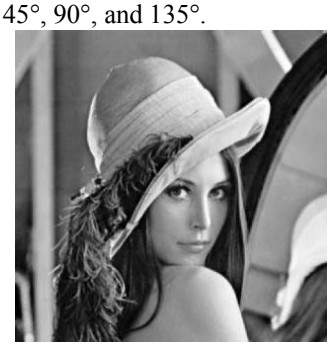

(a)

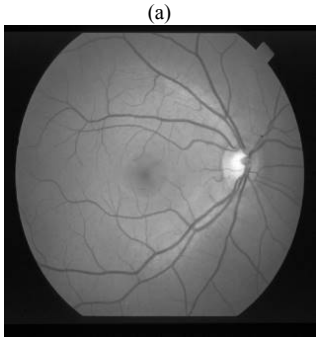

(b)

Figure 11. Test images: (a) Lena; (b) Retina

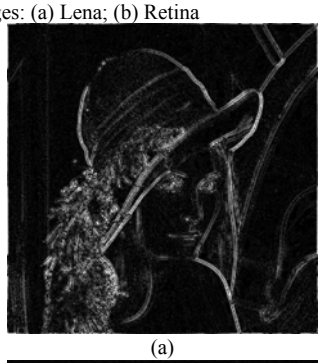

(a)

(b)

Figure 12. Test image responses with Gaussian high pass filters: (a) Lena; (b) Retina

Fig. 13 shows the results of the rose curve filter for different angles for the Lena image. As can be clearly seen, different angles extract different image features. The Lena image has edges in different directions, but the Lena image mainly contains edges lie at different than 0° and 90°. Fig. 13 shows features extracted from angles which were mentioned above. Especially, Fig. 13 (b) and Fig. 13 (d) show the performance of the proposed mechanism when angle is selected as 45° and 135°.

Especially in Fig. 13 (d), edges of Lena's hat were successfully extracted when the β parameter was selected as 135°. If other parameters such as leaf length or D_0 are changed, more features can be obtained.

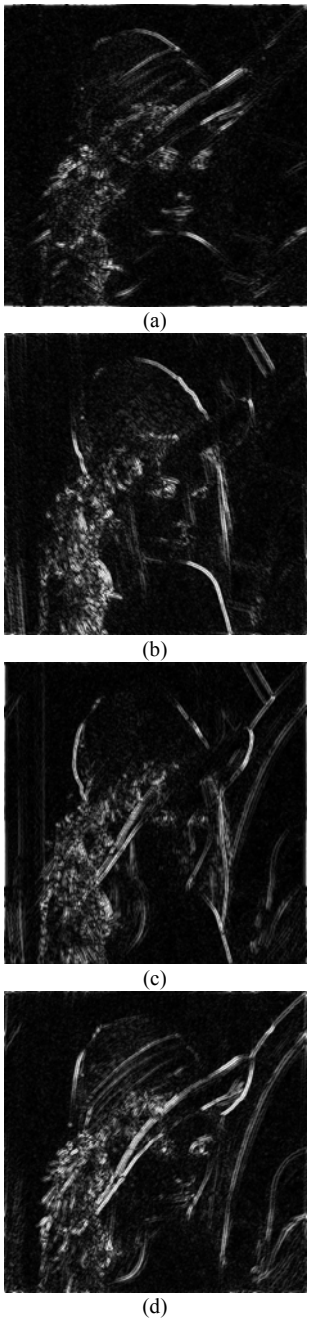

(a) (b) (c) (d)

Figure 13. Lemniscate filter bank responses for the Lena image: (a) β = 0° (b) β = 45° (c) β = 90° (d) β = 135°

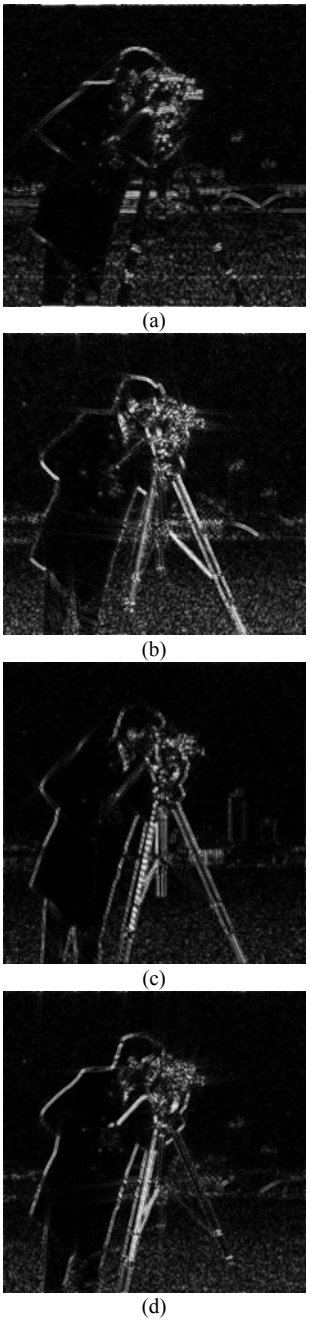

(a) (b) (c) (d)

Figure 14. Lemniscate filter bank responses for the Cameraman image: (a) β = 0° (b) β = 45° (c) β = 90° (d) β = 135°

Fig.14 shows the results for the Cameraman image using different angles for Lemniscate curves in the frequency domain. Different from the Lena image, the Cameraman image has edges which are more particular when angle is concern. Horizontal and vertical edges (Fig. 14(a), Fig. 14(c) respectively) extracted from the Cameraman image using proposed feature extraction mechanism are more obvious. Moreover, when angle of 45° and 135° are to be selected as β parameter, edges lie at these directions can be extracted successfully. This can be seen in Fig. 14(b) and Fig. 14(d). As can be seen from the directional edges in the image, any edges can be easily extracted using the desired angle β, as selected by the user.

Finally, to show the practical application of the filter, a retina image was also tested (Fig. 11(b)). The determination of blood vessels in retina images is especially important in biometric identification and glaucoma diagnosis.

Blood vessels are high-frequency components that can have different directions. Because the proposed filter for feature extraction process is steerable, it can easily extract blood vessels (Fig. 15).

These results show that the proposed filter can extract robust features at any angle.

As mentioned, this filter can extract more than one direction with a single filter.

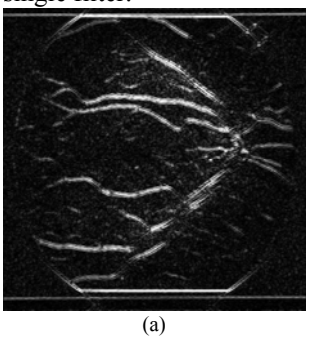

(a)

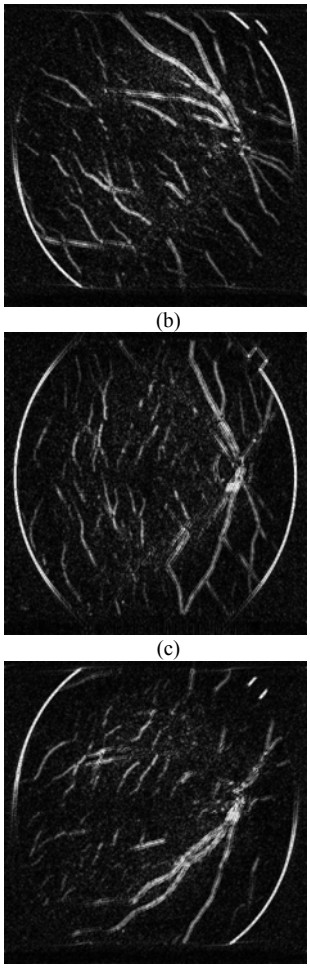

Figure 15. Lemniscate filter bank responses for the Retina image (a) $\beta = 0^{\circ}$ (b) $\beta = 45^{\circ}$ (c) $\beta = 90^{\circ}$ (d) $\beta = 135^{\circ}$

Generally, the Lemniscate has two symmetric leaves around the frequency plane origin. If the filter has four leaves, by setting coefficient of θ to 4 in (8), it can extract both horizontal and vertical features from the frequency domain (Fig. 16). The frequency response of a four-leaf Lemniscate is given in Fig. 17.

We applied the four-leaf Lemniscate to all three test images (Fig. 18) and this filter was able to extract both horizontal and vertical features. With a pre-processing step, more robust features could be extracted.

These results show that the rose curve filter used for feature extraction can extract features without being constrained by angle. It has many advantages such as directionality, control over the number of leaves, and a high pass radius which can easily be adjusted by the user. Its most distinguishing property is direction selectivity. Features at any angle can be extracted.

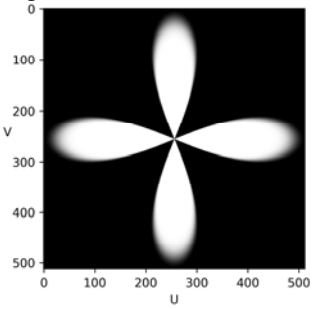

Figure 16. Four-leaf Lemniscate

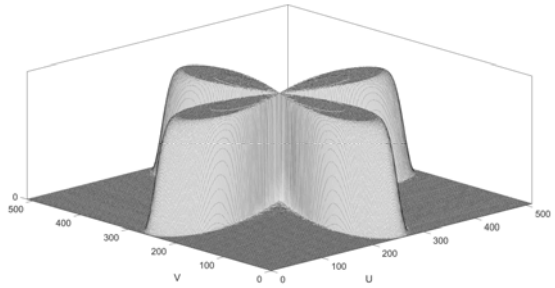

Figure 17. Frequency response of the proposed filter with four leaves

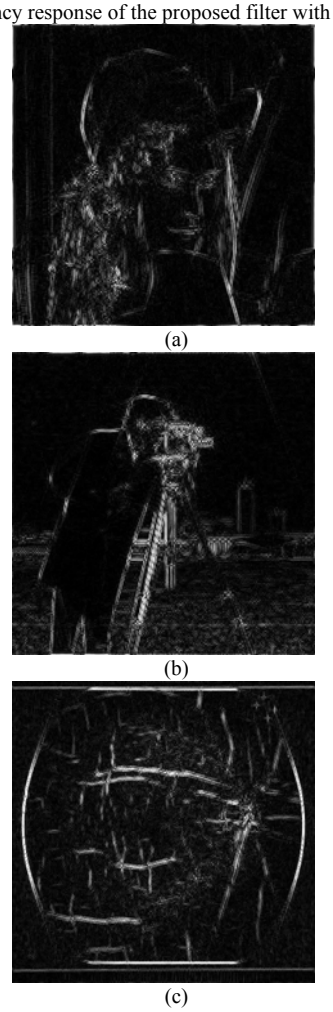

Figure 18. Lemniscate filter bank responses for images of (a) Lena, (b) the Cameraman, and (c) the Retina

The Gaussian high pass filter can be changed to the Butterworth filter. Moreover, it can be combined with the Laplacian Pyramid scheme, which is often used with the Contourlet transform to extract more robust features.

The proposed feature extraction mechanism is to be used with the original Lemniscate formula since it has two symmetric leaves around the origin. Moreover, when rotation parameter β changes, this symmetry does not change, and desired feature lie at certain angle can be extracted. However, when four-leaf version of Lemniscate is to be used, β parameter should not be changed. Four-leaf version of Lemniscate can extract features both horizontally and vertically when β parameter is selected as 0°. Nevertheless, if β parameter is set different from angle of 0°, all four-leaves will rotate, thus features other than selected angle will be extracted. In addition, as can be seen from the Fig. 16, leaves' width of rose curve will decrease as number

of leaf increases. For these specific reasons, original Lemniscate shape is to be used for feature extraction.

Another important parameter for the proposed feature extraction mechanism is leaf length (parameter a). For qualitative experiments, a was set to 256, half the height of the image. Since the Lemniscate is symmetrical, the filter can extract full horizontal or vertical features when the angle is set to 0° or 90° respectively. However, if leaf length is changed, different features can be obtained.

These properties make the rose curve suitable for feature extraction in the field of image processing. Since it has simple parameters, they can be easily controlled by the user.

B. Quantitative Performance

In order to evaluate the performance of the proposed filter for feature extraction quantitatively, the proposed mechanism with Lemniscate was tested on Facial Expression Recognition (FER) classification. In basic terms, a facial expression can be stated as the emergence of a feeling in a human face. Generally, typical facial expressions can be divided into 7 categories according to [30]. These expressions are: Anger, Disgust, Fear, Happiness, Sadness, Surprise, Neutrality.

Classification of these expressions can be divided into two categories; first one is Convolutional Neural Networks (CNN). Although user intervention in CNNs is minimal, CNNs suffer from myriad number of parameters which should be optimized. Second category concerning facial expression is to extract features from the faces by hand then feeding these features into any classification algorithm. However, when hand-crafted features are to be used, representing the expression good enough, in other words, extracting meaningful features is one of the problems, deciding parameters of the used filters to extract features from the faces is another problem.

Thus, using simplicity of the proposed feature extraction mechanism with Lemniscate filter type can be applied to facial expression classification.

1) Dataset

Publicly available CK+48 dataset contains 7 different facial emotions as mentioned above. An example face for each emotion is given in Fig. 19.

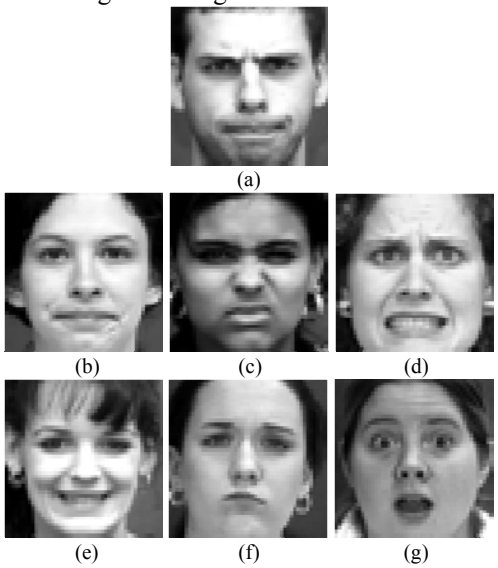

Figure 19. Examples of facial expressions: (a) Anger, (b) Contempt, (c) Disgust, (d) Fear, (e) Happy, (f) Sadness, (g) Surprise

As can be seen in Fig. 19, each expression contains different characteristics. Furthermore, if the images closely examined, we could easily see that main parts of an expression emerge in the region of eyes and mouths. To ground this view, each face in Fig. 19 is divided into two parts and given as in Fig. 20.

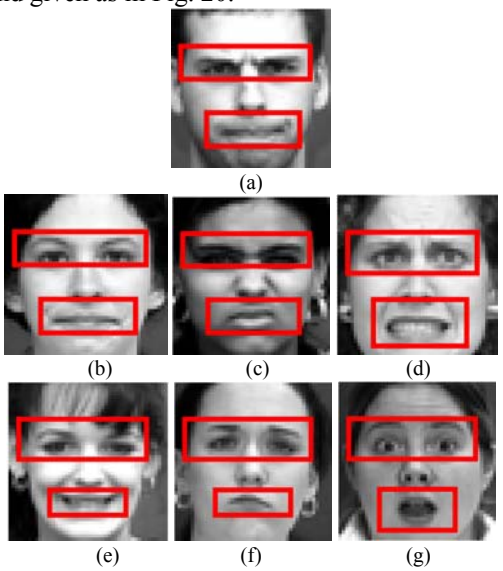

Figure 20. The most distinguishable parts in facial expressions: (a) Anger, (b) Contempt, (c) Disgust, (d) Fear, (e) Happy, (f) Sadness, (g) Surprise

All distinguishable features shown in Fig. 20, lies at certain angle, namely horizontal (0°). Since the proposed filter for feature extraction has the flexibility in angle selection, we can easily extract these features from frequency domain. Next section describes the method in feature extraction process.

2) Feature Extraction Method

As mentioned in previous section, regions that play important roles in facial expression is generally eyes and the mouths. In other words, extracting features from these two regions could successfully represent the expressions occur in the face.

Mentioned features lie horizontally in faces. Since proposed filter is flexible at angled features, mentioned features can be successfully extracted in frequency domain. Mentioned features can be extracted by the filter which is given in Fig. 21.

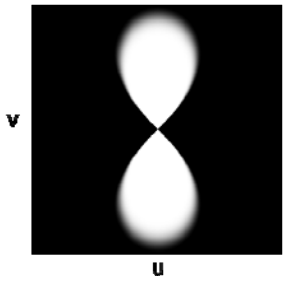

Figure 21. Proposed filter rotation in frequency domain to extract features

Before the feature extraction process, all images are resized into 64x64. Since the proposed filter for feature extraction process works in frequency domain and does not concern with the image size, simply, length parameter was selected as 32. To reduce the ringing effect problem, the proposed filter for feature extraction is used with Gaussian

High Pass Filter. As a high pass radius, the proposed filter was used with three different high pass radius sizes (35, 45, 55). Reason of three different high pass filters was to extract more discriminant features from the images which will be discussed shortly. Finally, we have only three filters that are ready to be used which are shown in Fig. 22.

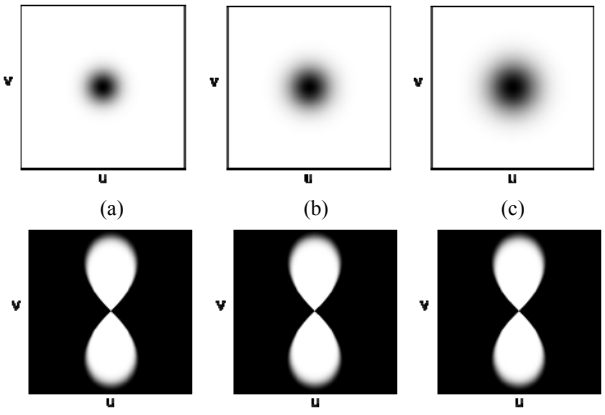

Figure 22. Prepared filters: (a) Gaussian High Pass Filter (D_0=35), (b) Gaussian High Pass Filter (D_0=45), (c) Gaussian High Pass Filter (D_0=55) (d,e,f) Proposed Filter Rotation with α=32, β = 0

Initially, the images were filtered with Gaussian High Pass Filter shown in Fig. 22 (a), then filtered with the proposed filter for feature extraction as shown in Fig. 22 (d) (Type I). Same procedure was applied again for Fig. 22 (b)-(e) (Type II) and Fig. 22 (c)-(f) (Type III). An example of features extracted from each expression is given in Fig. 23.

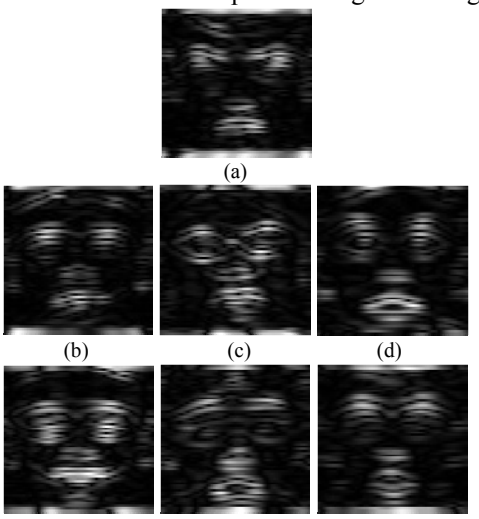

Figure 23. Features Extracted with the Proposed Method. (a) Anger, (b) Contempt, (c) Disgust, (d) Fear, (e) Happy, (f) Sadness, (g) Surprise

As for the reason of using three different filters with different high pass radiuses is to extract more robust features as for bigger radiuses means more higher frequencies (more sharp edges in spatial domain) can be extracted. This hypothesis can be seen in Fig. 24.

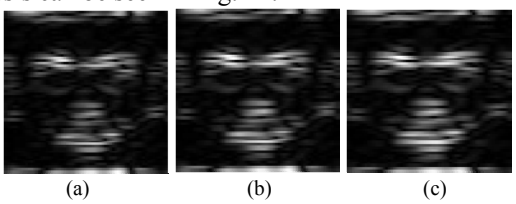

Figure 24. Effect of high pass radius. Emotion is Anger. (a) D_0=35, (b) D_0=45, (c) D_0=55

As can be seen from Fig. 23, horizontal features of the images were successfully extracted. Due to the curved shape of the proposed filter for feature extraction, curved features (especially eyebrows) can be extracted. As a person, we can successfully discriminate one expression from another expression. To automatically detect these expressions, these features were fed into machine learning algorithm and quantitatively analyzed. To see the effect of extracting higher frequencies in experiments, images alone filtered, and feature extracted by Type I, and features were fed into the algorithm. Then the features of the images were extracted by Type I and Type II combined, then were fed into the algorithm. Finally, the images' features were extracted by Type I, Type II and Type III were combined and were fed into the algorithm. Before feeding these features into algorithm, extracted features were flattened, and normalized between 0 and 1.

3) Experimental Results for Quantative Performance

In this study, Support Vector Machines (SVM) were selected as the machine learning algorithm [31]. The experiment was done by using Stratified K-Fold Cross Validation. The overall set were divided into 10-folds, and at each run 1-fold was removed for testing. And average accuracy (9) result of 10-folds cross validation was presented as a result. Also, average precision (10), average recall (11), and average F1 Score (12) were calculated. Results for average accuracy, average precision, average recall and average F1 Score were given in Table I.

$$Accuracy = \frac{TP + TN}{TP + TN + FP + FN} \tag{9}$$

$$Precision = \frac{TP}{TP + FP} \tag{10}$$

$$Recall = \frac{TP}{TP + FN} \tag{11}$$

$$F - Measure = \frac{2 \times precision \times recall}{precision + recall} \tag{12}$$

TP, TN, FP and FN denote the number of true positives, false positives, true negatives, and false negatives respectively.

TABLE I. RESULTS FOR PROPOSED METHOD

Filter(s) Used	Results	
Type I	Avg. Accuracy	%71.42
	Avg. Precision	%70.47
	Avg. Recall	%71.42
	Avg. F Measure	%68.47
Type I & Type II	Avg. Accuracy	%97.85
	Avg. Precision	%97.38
	Avg. Recall	%97.33
	Avg. F Measure	%97.85
Type I & Type II & Type III	Avg. Accuracy	%97.14
	Avg. Precision	%98.09
	Avg. Recall	%97.14
	Avg. F Measure	%96.95

As can be seen from the Table I, the proposed feature extraction mechanism achieves good results in classification of facial expressions. Although three types of filters were used for feature extraction, results suggest that features that were obtained by the combination of Type I and Type II does not differ from the Type I-Type II-Type III

combination. Moreover, in some metrics, Type I-Type II combination was higher than Type I-Type II-Type III. Main advantage of the proposed method is that we extracted the features which we needed only. In general, results suggest that proposed filter for feature extraction could extract meaningful features to be used in a machine learning prototype.

The proposed method uses only three parameters to extract features and achieved similar results according to feature extraction methods in the literature which require complex feature extraction mechanisms [32-33]. Another advantage of the proposed method is that features only lie at desired angle by using β parameter were extracted.

IV. Conclusion

Feature extraction is a vital part of image processing. As computer vision has become more important, so researchers have improved methods for extracting features. This paper shows the improved performance of a steerable filter, which could have a pivotal role. The simplicity of this filter is an important preferable reason for researchers and users. Focusing on these two aspects, we proposed a novel filter for feature extraction process.

The proposed method decreases the number of parameters to be selected for filters used in feature extraction process such as 2D Gabor Filter which consists high number of parameters (6 parameters). The proposed method uses only three parameters. Another problem that the proposed method solves is angle selectivity in frequency domain. By controlling the β parameter, user could select any region in frequency domain.

Proposed method was tested qualitatively on sample images, and results showed that desired features lie at certain angle were successfully extracted. The proposed method also tested quantitively in a FER classification problem and achieved acceptable results for the metrics that were calculated. This means that, using only three parameters, similar results as presented in the literature were achieved in FER classification. Overall, the proposed method showed that it is a robust schema.

As emphasized before, the rose curve filter has only three completely adjustable parameters: leaf length, cutting frequency of the high pass filter (Gaussian or Butterworth), and rotation angle. With only these three parameters, any region in the frequency domain can be scanned for feature extraction. Its characteristics and orientation can be controlled by the user. Also, with a four-leaf Lemniscate, both horizontal and vertical features can be extracted.

The proposed filter for feature extraction can also be used as a filter bank to extract more features and is suitable for use with optimization techniques such as the genetic algorithm.

References

[1] G. Kumar and P. K. Bhatia, “A detailed review of feature extraction in image processing systems,” in 2014 Fourth International Conference on Advanced Computing Communication Technologies, Feb. 2014, pp. 5–12. doi:10.1109/ACCT.2014.74

[2] S. Arivazhagan and L. Ganesan, “Texture classification using wavelet transform,” Pattern Recognition Letters, vol. 24, no. 9, pp. 1513–1521, Jun. 2003. doi:10.1016/S0167-8655(02)00390-2

[3] Yang Bai, Lihua Guo, Lianwen Jin and Qinghua Huang, "A novel feature extraction method using pyramid histogram of orientation gradients for smile recognition," 2009 16th IEEE International Conference on Image Processing (ICIP), Cairo, 2009, pp. 3305-3308. doi:10.1109/ICIP.2009.5413938

[4] Priyanka and D. Kumar, “Feature extraction and selection of kidney ultrasound images using GLCM and PCA,” Procedia Computer Science, vol. 167, pp. 1722–1731, Jan. 2020. doi:10.1016/j.procs.2020.03.382

[5] Wenshuo Gao, Xiaoguang Zhang, Lei Yang and Huizhong Liu, "An improved Sobel edge detection," 2010 3rd International Conference on Computer Science and Information Technology, Chengdu, 2010, pp. 67-71. doi:10.1109/ICCSIT.2010.5563693

[6] S. E. El-Khamy, M. Lotfy and N. El-Yamany, "A modified fuzzy Sobel edge detector," Proceedings of the Seventeenth National Radio Science Conference. 17th NRSC'2000 (IEEE Cat. No.00EX396), Minufiya, Egypt, 2000, pp. C32/1-C32/9. doi:10.1109/NRSC.2000.838961

[7] Q. Ying-Dong, C. Cheng-Song, C. San-Ben, and L. Jin-Quan, “A fast subpixel edge detection method using Sobel–Zernike moments operator,” Image and Vision Computing, vol. 23, no. 1, pp. 11–17, Jan. 2005. doi:10.1016/j.imavis.2004.07.003

[8] R. H. Bamberger and M. J. T. Smith, "A filter bank for the directional decomposition of images: theory and design," in IEEE Transactions on Signal Processing, vol. 40, no. 4, pp. 882-893, April 1992. doi:10.1109/78.127960

[9] S. Chakrabarti and S. K. Mitra, "Design of two-dimensional digital filters via spectral transformations," in Proceedings of the IEEE, vol. 65, no. 6, pp. 905-914, June 1977. doi:10.1109/PROC.1977.10588

[10] L. Harn and B. Shenoi, "Design of stable two-dimensional IIR filters using digital spectral transformations," in IEEE Transactions on Circuits and Systems, vol. 33, no. 5, pp. 483-490, May 1986. doi:10.1109/TCS.1986.1085949

[11] M. N. Do and M. Vetterli, "The contourlet transform: an efficient directional multiresolution image representation," in IEEE Transactions on Image Processing, vol. 14, no. 12, pp. 2091-2106, Dec. 2005. doi: 10.1109/TIP.2005.859376

[12] V. Velisavljevic, B. Beferull-Lozano, M. Vetterli, and P. L. Dragotti, “Directionlets: anisotropic multidirectional representation with separable filtering,” IEEE Transactions on Image Processing, vol. 15, no. 7, pp. 1916–1933, Jul. 2006. doi:10.1109/TIP.2006.877076

[13] N. Ito, “Efficient design of two-dimensional diamond-shaped filters,” in 2010 International Symposium on Intelligent Signal Processing and Communication Systems, Dec. 2010, pp. 1–4. doi:10.1109/ISPACS.2010.5704647.

[14] D. V. Tosic, A. Mojsilovic, and M. Popovic, “Symbolic approach to 2D biorthogonal diamond-shaped filter design,” in 1997 21st International Conference on Microelectronics. Proceedings, Sep. 1997, vol. 2, pp. 709–712 vol. 2. doi:10.1109/ICMEL.1997.632943

[15] J. Ma and G. Plonka, “The curvelet transform,” IEEE Signal Processing Magazine, vol. 27, no. 2, pp. 118–133, Mar. 2010. doi:10.1109/MSP.2009.935453

[16] A. Ebrahimzadeh, “An efficient technique for classification of electrocardiogram signals,” Adv. Electr. Comp. Eng., vol. 9, no. 3, Art. no. 3, Oct. 2009. doi:10.4316/AECE.2009.03016

[17] Y. Liu, C. Zhang, J. Cheng, X. Chen, and Z. J. Wang, “A multi-scale data fusion framework for bone age assessment with convolutional neural networks,” Computers in Biology and Medicine, vol. 108, pp. 161–173, May 2019. doi:10.1016/j.compbiomed.2019.03.015

[18] N. G. Chitaliya and A. I. Trivedi, “An efficient method for face feature extraction and recognition based on contourlet transforms and principal component analysis,” Procedia Computer Science, vol. 2, pp. 52–61, Jan. 2010. doi:10.1016/j.procs.2010.11.008

[19] M. Yin, W. Liu, X. Zhao, Q.-W. Guo, and R.-F. Bai, “Image denoising using trivariate prior model in nonsubsampled dual-tree complex contourlet transform domain and non-local means filter in spatial domain,” Optik, vol. 124, no. 24, pp. 6896–6904, Dec. 2013. doi:10.1016/j.ijleo.2013.05.132

[20] D. Li, L. Zhang, J. Yang, and W. Su, “Research on wavelet-based contourlet transform algorithm for adaptive optics image denoising,” Optik, vol. 127, no. 12, pp. 5029–5034, Jun. 2016. doi:10.1016/j.ijleo.2016.02.042

[21] D. Guo and J. Chen, “The application of contourlet transform to image denoising,” Procedia Engineering, vol. 15, pp. 2333–2338, Dec. 2011. doi:10.1016/j.proeng.2011.08.437

[22] L. Li, X. Yuan, Z. Lu, and J.-S. Pan, “Rotation invariant watermark embedding based on scale-adapted characteristic regions,” Information Sciences, vol. 180, no. 15, pp. 2875–2888, Aug. 2010. doi:10.1016/j.ins.2010.04.009

[23] S. Etemad and M. Amirmazlaghani, "A new multiplicative watermark detector in the contourlet domain using t Location-Scale distribution," Pattern Recognition, vol. 77, pp. 99–112, May 2018. doi:10.1016/j.patcog.2017.12.006

[24] Y. Chen, J. Xiong, H. Liu, and Q. Fan, "Fusion method of infrared and visible images based on neighborhood characteristic and regionalization in NSCT domain," Optik, vol. 125, no. 17, pp. 4980–4984, Sep. 2014. doi:10.1016/j.ijleo.2014.04.006

[25] X. Yang, W. Xu, R. Luo, X. Zheng, and K. Liu, "Robustly reconstructing magnetic resonance images via structure decomposition," Magnetic Resonance Imaging, vol. 57, pp. 165–175, Apr. 2019. doi:10.1016/j.mri.2018.11.020

[26] Ö. Mintemur, R. Demirci, and H. Kaya, "Directional image filter using rose curve in frequency domain," in 2019 3rd International Symposium on Multidisciplinary Studies and Innovative Technologies (ISMSIT), Oct. 2019, pp. 1–4. doi:10.1109/ISMSIT.2019.8932887

[27] E. J. Wood, "Applying Fourier and associated transforms to pattern characterization in textiles," Textile Research Journal, vol. 60, no. 4, pp. 212–220, Apr. 1990. doi:10.1177/004051759006000404

[28] J. G. Daugman, "Uncertainty relation for resolution in space, spatial frequency, and orientation optimized by two-dimensional visual cortical filters," J. Opt. Soc. Am. A, JOSAA, vol. 2, no. 7, pp. 1160–1169, Jul. 1985. doi:10.1364/JOSAA.2.001160

[29] Y. Yuan, J. Zhang, and Q. Wang, "Deep Gabor convolution network for person re-identification," Neurocomputing, vol. 378, pp. 387–398, Feb. 2020. doi:10.1016/j.neucom.2019.10.083

[30] X. Sun, P. Xia, L. Zhang, and L. Shao, "A ROI-guided deep architecture for robust facial expressions recognition," Information Sciences, vol. 522, pp. 35–48, Jun. 2020. doi:10.1016/j.ins.2020.02.047

[31] I. Dagher, E. Dahdah, and M. Al Shakik, "Facial expression recognition using three-stage support vector machines," Vis Comput Ind Biomed Art, vol. 2, no. 1, p. 24, Dec. 2019. doi:10.1186/s42492-019-0034-5

[32] R. R. K. Dewi, F. Sthevanie, and A. Arifianto, "Face expression recognition using Local Gabor Binary Pattern Three Orthogonal Planes (LGBP-TOP) and Support Vector Machine (SVM) method," J. Phys.: Conf. Ser., vol. 1192, p. 012048, Mar. 2019. doi:10.1088/1742-6596/1192/1/012048

[33] Y. Sun and J. Yu, "Facial expression recognition by fusing Gabor and Local Binary Pattern features," in MultiMedia Modeling, Cham, 2017, pp. 209–220. doi:10.1007/978-3-319-51814-5_18